Engineering with Computers (2012) 28:189–198
DOI 10.1007/s00366-011-0237-7

ORIGINAL ARTICLE

Separation of CO_2 by single and mixed aqueous amine solvents in membrane contactors: fluid flow and mass transfer modeling

Saeed Shirazian · Azam Marjani · Mashallah Rezakazemi

Received: 29 March 2011 / Accepted: 21 June 2011 / Published online: 8 July 2011

Abstract Removal of carbon dioxide from gas mixtures is of vital importance for the control of greenhouse gas emission. This study presents a numerical simulation using computational fluid dynamics of mass and momentum transfer in hollow-fiber membrane contactors. The simulation was conducted for physical and chemical absorption of CO_2. A mass transfer model was developed to study CO_2 transport through hollow-fiber membrane contactors. The model considers axial and radial diffusions in the contactor. It also considers convection in the tube and shell side with chemical reaction. The model equations were solved by numerical method based on finite element method. Moreover, the simulation results were validated with the experimental data obtained from literature for absorption of CO_2 in amine aqueous solutions as solvent. The simulation results were in good agreement with the experimental data for different values of gas and liquid velocities. The simulation results indicated that the removal of CO_2 increased with increasing liquid velocity in the tube side. Simulation results also showed that hollow-fiber membrane contactors have a great potential in the area of gas separation specially CO_2 separation from gas mixtures.

Keywords Gas separation · Membrane contactor · CFD · Numerical simulation · Mass transfer

List of symbols

A	Cross-section of shell (m^2)
C_0	Inlet CO_2 concentration (mol/m^3)
C	Concentration (mol/m^3)
$C_{CO_2-membrane}$	CO_2 concentration in the membrane (mol/m^3)
$C_{CO_2-shell}$	CO_2 concentration in the shell (mol/m^3)
C_{CO_2-tube}	CO_2 concentration in the tube (mol/m^3)
C_i	Concentration of any species (mol/m^3)
$C_{i\text{-shell}}$	Concentration of any species in the shell (m^2/s)
C_{in}	Absorbent concentration at the inlet (mol/m^3)
C_{inlet}	Inlet concentration of CO_2 in the shell (mol/m^3)
C_{outlet}	Outlet concentration of CO_2 in the shell (mol/m^3)
D	Diffusion coefficient (m^2/s)
$D_{CO_2-membrane}$	Diffusion coefficient of CO_2 in the membrane (m^2/s)
D_{CO_2-tube}	Diffusion coefficient of CO_2 in the tube (m^2/s)
$D_{i\text{-shell}}$	Diffusion coefficient of any species in the shell (m^2/s)
J_i	Diffusive flux of any species (mol/m^2 s)
J_{CO_2}	Mass transfer rate of CO_2 ($mol/(m^2$ s))
k	Reaction rate coefficient of CO_2 with absorbent (m^3/mol s)
L	Length of the fiber (m)
m	Physical solubility (–)
n	Number of fibers
P	Pressure (Pa)
Q_{shell}	Gas flow rate (ml/min)
Q_{tube}	Liquid flow rate (ml/min)
r_1	Tube inner radius (m)
r_2	Tube outer radius (m)
r_3	Shell inner radius (m)
r	Radial coordinate (m)

S. Shirazian · A. Marjani (✉) · M. Rezakazemi
Department of Chemistry, Islamic Azad University, Arak Branch, Arak, Iran
e-mail: a-marjani@iau-arak.ac.ir

R	Module inner radius (m)
R_i	Overall reaction rate of any species (mol/m^3 s)
Re	Reynolds number (–)
t	Time (s)
T	Temperature (K)
T_l	Liquid temperature (K)
T_g	Gas temperature (K)
u	Average velocity (m/s)
U_g	Gas velocity (m/s)
U_l	Liquid velocity (m/s)
V	Velocity in the module (m/s)
$V_{z\text{-shell}}$	Z velocity in the shell (m/s)
$V_{z\text{-tube}}$	Z velocity in the tube (m/s)
x_p	Constant used in (29) (–)
x_w	Constant used in (30) (–)
z	Axial coordinate (m)

Greek symbols

ε	Porosity
v	Volumetric flow rate (m^3/s)
τ	Tortuosity
ϕ	Module volume fraction
α	Loading of CO_2 in amine (kmol of CO_2/kmol of amine)
η	CO_2 removal efficiency
η	Gas viscosity (Pa.s)
ρ	Density (kg/m^3)

1 Introduction

Nowadays, reduction of greenhouse gases is a subject of great interest in the field of environment. Greenhouse gases cause global warming, which in turn results in serious environmental problems [1]. Carbon dioxide is the main greenhouse gas and constitutes about 80% of greenhouse gases. It is reported that half of the CO_2 emissions are produced by industry and power plants using fossil fuels [2]. The CO_2 concentrations are typically 3–5% in gas-fired power plants and 13–15% in coal plants [3].

At the moment, carbon dioxide removal technologies are based on a variety of physical and chemical processes, including, absorption, adsorption, cryogenic and membrane techniques [4]. Conventional processes for the separation of CO_2 suffer from some problems, such as flooding, foaming, entraining, channeling, and high capital and operating costs. Therefore, many studies have been conducted to enhance the efficiency of these processes to reduce their problems. Hollow-fiber membrane contactors (HFMCs) are expected to overcome the disadvantages of the conventional equipment for gas separation [4]. The main characteristic of HFMCs is that the gas stream flows

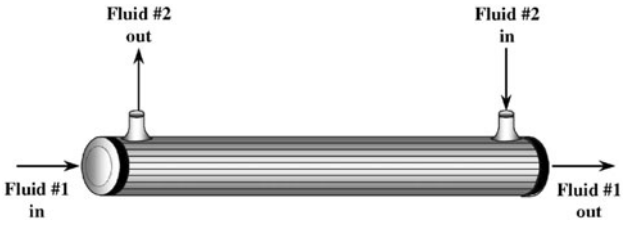

Fig. 1 A parallel flow hollow-fiber membrane module [24]

on one side and the chemical solvent flows on the other side of the membrane without phase dispersion, thus avoiding the problems often encountered in the conventional equipment such as flooding, foaming, channeling and entrainment. Figure 1 shows a parallel hollow-fiber membrane module.

Some experiments and theories about the HFMCs have been done since Zhang and Cussler first studied these contactors [5]. Using polypropylene hollow fibers, Kreulen et al. [6] studied absorption of CO_2 into water/glycerol mixtures. The authors studied the hollow-fiber membrane as gas–liquid contactors in the case of both physical and chemical absorption. Falk-Pederson and Dannstrom [7] studied separation of CO_2 from offshore gas using HFMCs and optimized the process with respect to sizes, weight and costs. Some researchers have reported the use of HFMCs for absorption of CO_2 in a hydroxide solution [8] and the CO_2 capture in membrane using amino acid salts [9]. Qi and Cussler [5] studied development of a theory of the operation of HFMCs and calculated mass transfer coefficients in liquid phase. They also obtained the overall mass transfer coefficients, including resistances in both liquid and membrane, and compared the performance of hollow fibers with that of packed towers.

Separation of CO_2 and SO_2 from CO_2/N_2 and SO_2/air gas mixtures using water in a parallel module was studied by Karoor and Sirkar [10]. They utilized microporous polypropylene hollow fibers as contactor. A similar study has been recently conducted by Zhang et al. [11] for co-current gas–liquid contact. Kim and Yang [12] investigated the separation of CO_2/N_2 mixtures using HFMCs theoretically and experimentally. They developed a mass transfer model integrating 3 mass transfer resistances in series. Although there was an agreement between the model predictions with experimental data, they assumed a linear decrease in gas flow rate for the simulation purpose, which is not a good assumption at high velocities.

All theoretical studies have focused on resistances-in-series model. This model needs mass transfer coefficients to be estimated experimentally. A mass transfer model that can provide a general simulation of the chemical and physical absorption in HFMCs is of vital importance for designing these contactors. This study focuses on

simulation of carbon dioxide absorption in a hollow-fiber membrane module. Axial and radial diffusions in all sides of the membrane contactor are considered in the mass transfer equations. The aim of the simulation is to predict the concentration of gas components in the membrane contactor. The influence of various process parameters on the mass transfer of CO_2 is then investigated. Chemical absorption for "non-wetted mode" is considered in this work. For the non-wetted mode, the membrane pores are filled with gas mixture because the membrane nature is hydrophobic and the pressure difference of liquid–gas does not exceed the critical pressure. Many researchers indicate that the non-wetted operation is preferably during absorption because mass transfer coefficient in non-wetted mode is much higher than that in wetted mode [6]. Therefore, it is always desired that the absorption process is non-wetted mode operation. Chemical absorption is considered for absorption of CO_2 in aqueous solution of amines. The model is then validated using experimental data obtained from literature for the absorption of CO_2 in amine aqueous solutions.

2 Model developments

A comprehensive two-dimensional mathematical model was developed for the transport of carbon dioxide through HFMCs. In this work, the separation of CO_2 from CO_2/N_2 gas mixture using amines aqueous solutions (MEA & MDEA) as absorbents in HFMCs is studied. The model was based on "non-wetted mode" in which the gas mixture filled the membrane pores for countercurrent gas–liquid contacts. Laminar parabolic velocity distribution was used for the liquid flow in the tube side, whereas the gas flow in the shell side was characterized by solving Navier–Stokes equations. Axial and radial diffusions inside the fiber, through the membrane, and within the shell side of the contactor were considered in the equations. The membrane considered in this study is hydrophobic; therefore, liquid phase cannot penetrate the membrane pores, and membrane is filled by gas.

2.1 Model equations

A mass transfer model is developed for a hollow fiber, as shown in Fig. 2. The gas mixture (CO_2 and N_2) flows with a fully developed laminar velocity in the shell side, and the liquid absorbent (MEA or MDEA) flows with laminar flow in the tube side. Based on Happel's free surface model [13], only portion of fluid surrounding the fiber is considered and may be approximated as circular cross-section. Therefore, the HFMC consists of three sections: tube side, membrane and shell side. The steady-state two-dimensional mass balances are carried out for all three sections.

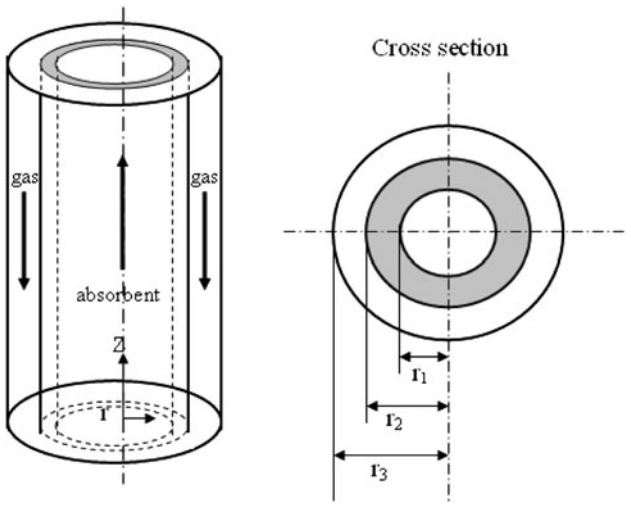

Fig. 2 Model domain (axial symmetry). Three sections of membrane contactor

The gas mixture is fed to the shell side (at $z = L$), while the absorbent is passed through the tube side (at $z = 0$). CO_2 is removed from the gas mixture by diffusing through the membrane pores and then is absorbed in the solvent.

The model is built considering the following assumptions:

1. steady-state and isothermal conditions.
2. fully developed parabolic liquid velocity profile in the hollow fiber.
3. ideal gas behavior is imposed.
4. the Henry's law is applicable for gas–liquid interface.
5. laminar flow for gas and liquid flow in the contactor.
6. non-wetted mode in which the gas mixture filled the membrane pores and the liquid absorbent cannot wet membrane pores.

2.1.1 *Shell side equations*

The continuity equation for each species in a reactive absorption system can be expressed as [14]:

$$\frac{\partial C_i}{\partial t} = -(\nabla \cdot C_i V) - (\nabla \cdot J_i) + R_i \quad (1)$$

where C_i, J_i, R_i, V and t are the concentration, diffusive flux, reaction rate of species i, velocity and time, respectively. Either Fick's law of diffusion or Maxwell–Stefan theory can be used for the determination of diffusive fluxes of species i.

The continuity equation for steady state for CO_2 in the shell side of contactor for cylindrical coordinate is obtained using Fick's law of diffusion for estimation of diffusive flux:

$$D_{CO_2-shell}\left[\frac{\partial^2 C_{CO_2-shell}}{\partial r^2}+\frac{1}{r}\frac{\partial C_{CO_2-shell}}{\partial r}+\frac{\partial^2 C_{CO_2-shell}}{\partial z^2}\right] = V_{z-shell}\frac{\partial C_{CO_2-shell}}{\partial z} \quad (2)$$

In this equation, we consider diffusion mass transfer with respect to r and z directions, and we only consider convective mass transfer with respect to z direction because we assume fluids inside the membrane contactor flow in axis (z) direction and there is no flow in r direction. The fluid velocity in r direction is neglected, and mass transfer in r direction occurs slowly. It is notable that the chemical reaction is not considered in the shell side.

We use the Navier–Stokes equations to characterize the shell-side velocity. In laminar flow, the Navier–Stokes equations apply [14]:

$$\begin{aligned} &-\eta\Delta V+\rho(V\cdot\nabla)V+\nabla p=0\\ &\nabla\cdot V=0 \end{aligned} \quad (3)$$

The gas flow in the shell side of the membrane contactor can be configured as fluid envelop around the fiber, and there is no interaction between hollow fibers. The dimension of the free surface can be estimated by Happel's free surface model [13]:

$$r_3=\left(\frac{1}{1-\phi}\right)^{1/2} r_2 \quad (4)$$

in which ϕ is the volume fraction of the void. It can be calculated as follows [13]:

$$1-\phi=\frac{nr_2^2}{R^2} \quad (5)$$

where n is the number of fibers and R is the module inner radius.

Boundary conditions for shell side are given as:

$$\text{at}\quad z=L,\quad C_{CO_2-shell}=C_0,\quad V_z=V_{in}\quad \text{(Inlet boundary)} \quad (6)$$

$$\text{at}\quad r=r_3,\quad \frac{\partial C_{CO_2-shell}}{\partial r}=0\,\text{(Insulation boundary)},\quad V_z=0\,\text{(No-slip condition)} \quad (7)$$

$$\text{at}\quad r=r_2,\quad C_{CO_2-shell}=C_{CO_2-membrane},\quad V_z=0\,\text{(No-slip condition)} \quad (8)$$

At the outlet of shell side ($z = 0$), we assume that the convective contribution to the mass transport is much larger than the diffusive contribution:

$$\text{at}\quad z=0,\quad (-D\nabla C_{CO_2-shell}+C_{CO_2-shell}V)=C_{CO_2-shell}V \quad (9)$$

Laminar flow is obtained on the shell side, if the Reynolds number calculated at the outlet of the shell side is such that $Re_{out} < 4.000$ [14]. The Reynolds number is calculated from equation for annulus given by [14]:

$$Re_{out}=\frac{2r_3\rho V_{out}(1-\frac{r_2}{r_3})}{\eta} \quad (10)$$

where V_{out} is the mean fluid velocity at the outlet of the shell side. The density and the viscosity data are those of nitrogen at 25°C ($\rho = 1.14$ kg/m^3 and $\eta = 17.84 \times 10^{-6}$ Pa.s [19]) because the concentration of CO_2 in gas mixture is low (about 10%) and we neglect it in calculation of density and viscosity for gas mixture. The mean velocity at the outlet is obtained from integrating the local velocity at outlet of shell side ($z = 0$):

$$V_{out}=\frac{\iint_{Z=0}V(r)\mathrm{d}A}{\iint_{Z=0}\mathrm{d}A} \quad (11)$$

2.1.2 Membrane equations

The steady-state continuity equation for the transport of CO_2 inside the membrane, which is considered to be due to diffusion alone, may be written as:

$$D_{CO_2-membrane}\left[\frac{\partial^2 C_{CO_2-membrane}}{\partial r^2}+\frac{1}{r}\frac{\partial C_{CO_2-membrane}}{\partial r}+\frac{\partial^2 C_{CO_2-membrane}}{\partial z^2}\right]=0 \quad (12)$$

Boundary conditions are given as:

$$\text{at}\quad r=r_2,\quad C_{CO_2-membrane}=C_{CO_2-shell} \quad (13)$$

$$\text{at}\quad r=r_1,\quad C_{CO_2-membrane}=C_{CO_2-tube}/m \quad (14)$$

where m is the solubility of CO_2 in the solution.

We also assume symmetry condition at the horizontal boundaries of the membrane side:

$$\text{at}\quad z=0,\quad (-D\nabla c_{CO_2-membrane})=0 \quad (15)$$

$$\text{at}\quad z=L,\quad (-D\nabla c_{CO_2-membrane})=0 \quad (16)$$

Gas absorption membranes are microporous, and they are homogeneous in pores. Membrane area is treated as a quasi-homogeneous medium. Membrane material is microporous, so there is no concentration difference between the membrane and shell side at the interface. In these contactors, the membrane mainly acts as a physical barrier between two phases without significant effect in terms of selectivity.

2.1.3 Tube side equations

The steady-state continuity equation for the transport with chemical reaction of CO_2 and absorbent in the tube side, where CO_2 is absorbed and reacts with solvent, may be written as:

$$D_{\text{i-tube}}\left[\frac{\partial^2 C_{\text{i-tube}}}{\partial r^2}+\frac{1}{r}\frac{\partial C_{\text{i-tube}}}{\partial r}+\frac{\partial^2 C_{\text{i-tube}}}{\partial z^2}\right] = V_{\text{z-tube}}\frac{\partial C_{\text{i-tube}}}{\partial z}-R_{\text{i}} \quad (17)$$

where i refers to CO_2 or absorbent and R_i is reaction rate between CO_2 and absorbent.

The velocity distribution in the tube is assumed to follow Newtonian laminar flow [14]:

$$V_{\text{z-tube}} = 2u\left[1-\left(\frac{r}{r_1}\right)^2\right] \quad (18)$$

where u is average velocity in the tube side.

Boundary conditions for tube side:

$$\text{at} \quad z=0, \quad C_{\text{CO}_2\text{-tube}}=0, \quad C_{\text{absorbent}}=C_{\text{in}} \quad (19)$$

$$\text{at} \quad r=r_1, \quad C_{\text{CO}_2\text{-tube}}=m\times C_{\text{CO}_2\text{-membrane}}, \quad \frac{\partial C_{\text{absorbent-tube}}}{\partial r}=0 \quad \text{(non-wetted mode)} \quad (20)$$

$$\text{at} \quad r=0, \quad \frac{\partial C_{\text{CO}_2\text{-tube}}}{\partial r}=\frac{\partial C_{\text{absorbent-tube}}}{\partial r}=0 \quad \text{(symmetry)} \quad (21)$$

At the outlet of tube side ($z = L$), we assume again that the convective contribution to the mass transport is much larger than the diffusive contribution:

$$\text{at } z=L, \quad \left(-D\nabla C_{\text{CO}_2\text{-tube}}+C_{\text{CO}_2\text{-tube}}V_{\text{z-tube}}\right)=C_{\text{CO}_2\text{-tube}}V_{\text{z-tube}} \quad (22)$$

2.1.3.1 Reaction rate for CO_2 absorption into amine aqueous solutions Two typical amine aqueous solutions of monoethanolamine (MEA) and methyldiethanol amine (MDEA) were used as absorbent in this study. The zwitterions mechanism was adopted for the reaction of CO_2 with primary or secondary alkanolamines [15]:

$$\text{CO}_2+R_1R_2\text{NH}\overset{k_1}{\leftrightarrow}R_1R_2\text{NH}^+\text{COO}^- \quad (23)$$

$$R_1R_2\text{NH}^+\text{COO}^-+B\xrightarrow{k_b}R_1R_2\text{NCOO}^-+\text{BH}^+ \quad (24)$$

where R_1 is an alkyl and R_2 is H for primary amines and an alkyl for secondary amines, B is a base that could be an amine, OH, or H_2O. For this mechanism, the reaction rate of CO_2 with MEA can be expressed as follows [16]:

$$R_{\text{CO}_2\text{-MEA}}=\frac{k_{1,\text{MEA}}C_{\text{CO}_2}C_{\text{MEA}}}{1+\frac{k_{-1}}{k_{\text{H}_2\text{O}}C_{\text{H}_2\text{O}}+k_{\text{OH}^-1}C_{\text{OH}^-1}+k_{\text{MEA}}C_{\text{MEA}}+k_{\text{MDEA}}C_{\text{MDEA}}}} \quad (25)$$

The reaction kinetics for the reaction of carbon dioxide with MDEA aqueous has been studied extensively. All the data for CO_2 with MDEA are in agreement well with the pseudo-first-order reaction [15–18]:

$$R_{\text{CO}_2\text{-MDEA}}=k_{2,\text{MDEA}}C_{\text{CO}_2}C_{\text{MDEA}} \quad (26)$$

The reaction kinetics for the reaction of CO_2 with H_2O can be expressed as follows [15]:

$$R=R_{\text{CO}_2\text{-OH}^-}+R_{\text{CO}_2\text{-H}_2\text{O}} \quad (27)$$

The reaction of CO_2 with H_2O can be negligible due to the weak contribution [15].

The reaction of CO_2 with hydroxyl ion can be described as [17]:

$$R_{\text{CO}_2\text{-OH}^-}=k_{\text{OH}^-}C_{\text{CO}_2}C_{\text{OH}^-} \quad (28)$$

$$C_{\text{OH}^-}=\frac{x_w}{x_p}\left(\frac{1-\alpha}{\alpha}\right), \quad \alpha\geq 10^{-3} \quad (29)$$

$$C_{\text{OH}^-}=\sqrt{\frac{x_w}{x_p}C_{amine}}, \quad \alpha<10^{-3} \quad (30)$$

where α is the CO_2 loading in amine solution. The value of x_w and x_p is given in Table 1.

2.2 Numerical solution of the model equations

The model equations with the boundary conditions were solved numerically using COMSOL software. This package uses finite element method (FEM) for numerical solutions of differential equations. The finite element analysis is combined with adaptive meshing and error control using numerical solver of UMFPACK. This solver is well suited for solving stiff and non-stiff non-linear boundary value problems. An IBM-PC-Pentium4 (CPU speed is 2,800 MHz) was used to solve the set of equations. The computational time for solving the set of equations was about 38 min.

Figure 3 shows a segment of the mesh used to determine the gas transport behavior in hollow-fiber membrane contactor (HFMC). It should be pointed out that the COMSOL mesh generator creates tetrahedral mesh that is isotropic in size. A large number of elements are then created with scaling. A scaling factor of 800 (the fiber length is 800 mm) has been employed in z direction due to large difference between r and Z. COMSOL automatically scales back the geometry after meshing. This generates an anisotropic mesh around 1,065 elements.

3 Results and discussion

3.1 Concentration distribution of CO_2 in the contactor

Dimensionless concentration distribution of CO_2 in the tube, membrane and shell side of the membrane contactor is illustrated in Fig. 4. As it is seen from the figure, the gas

Table 1 Parameters used in simulation for CO_2 absorption into amines aqueous solutions

Parameter	Value
D_{CO_2/N_2} (25°C, 121.3 kPa)	1.39×10^{-5} m^2 s^{-1} [20]
$D_{CO_2/MDEA}$ (25°C, 10 wt. % MDEA)	1.63×10^{-9} m^2 s^{-1} [21]
$D_{MDEA/Solution}$ (25°C, 10 wt. % MDEA)	6.91×10^{-10} m^2 s^{-1} [22]
$D_{MEA/Solution}$ (25°C, 10 wt. % MDEA)	1.09×10^{-10} m^2 s^{-1} [22]
$D_{CO_2/Membrane}$ (25°C, 1 atm)	3.38×10^{-6} [14]
x_w	$10^{-22.795+0.0294T}$ [18]
x_p	$10^{-14.123+0.01842T}$ [18]
$k_{2,MDEA}$	1.34×10^6 exp (−5,771/T) m^3 mol^{-1} s^{-1} [17]
$k_{1,MEA}$	7.973×10^9 exp (−6,243/T) m^3 mol^{-1} s^{-1} [18]
k_{OH^-}	$10^{13.625-2895/T}$ m^3 $kmol^{-1}$ s^{-1} [18]
$k_{1,MEA}$ k_{H_2O}/k_{-1}	1.1 exp (−3,472/T) m^6 mol^{-2} s^{-1} [18]
$k_{1,MEA}$ k_{MEA}/k_{-1}	1.563×10^8 exp (−7,544/T) m^6 mol^{-2} s^{-1} [18]
$k_{1,MEA}$ k_{MDEA}/k_{-1}	86.76 exp (−3,637/T) m^6 mol^{-2} s^{-1} [18]
Henry constant of CO_2 with aqueous (25°C, 10% MDEA)	0.891 [22]

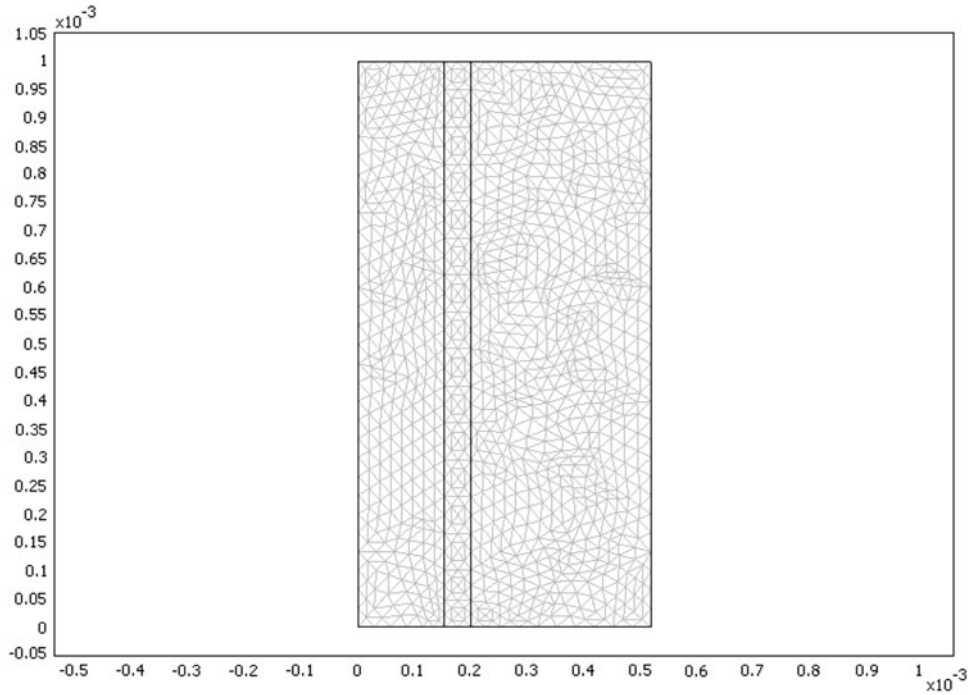

Fig. 3 Magnified segment of the mesh used in the numerical simulation. There are 1,065 elements in total for the whole HFMC domain. z Direction scale factor = 800. The three domains from left to right are fiber side, membrane and shell, respectively

mixture containing CO_2 and N_2 flows from one side of the membrane contactor ($z = L$) where the concentration of CO_2 is the highest (C_0). On the other hand, the chemical solvent (MDEA) flows from the other side ($z = 0$) where the concentration of CO_2 is assumed to be zero. As the gas flows through the shell side, it is transferred toward the membrane interface due to concentration difference that is the driving force for mass transfer of CO_2. CO_2 is transferred in the membrane contactor by two mass transfer mechanisms, including diffusion and convection. CO_2 is then absorbed by the moving solvent and swept by the solvent flow.

3.2 Effect of liquid flow rate on the separation of CO_2

The percentage removal of CO_2 can be calculated from the equation below:

$$\%\ \text{removal}\ CO_2 = 100\frac{(v \times C)_{inlet} - (v \times C)_{Outlet}}{(v \times C)_{inlet}} = 100\left(1 - \frac{C_{outlet}}{C_{inlet}}\right) \quad (31)$$

where v and C are the volumetric flow rate and concentration, respectively. C_{outlet} is calculated by integrating the local concentration at outlet of shell side ($z = 0$):

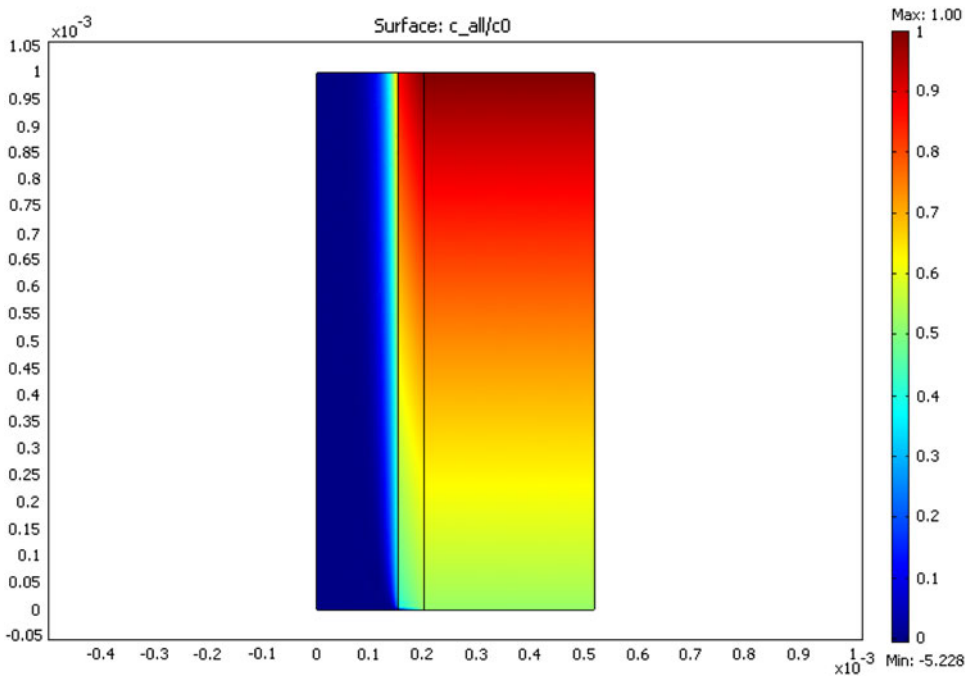

Fig. 4 A representation of the concentration distribution of CO_2 (C/C_0) in the membrane contactor for the absorption of CO_2 in MDEA. Gas flow rate = liquid flow rate = 100 ml/min; CO_2 inlet concentration = 10% vol.; amine (MDEA) inlet concentration = 10% wt; $n = 100$; $R = 0.5$ cm, $r_1 = 0.15$ mm, $r_2 = 0.20$ mm, $r_3 = 0.52$ mm, $L = 80$ cm, $Re_{out} = 3{,}500$

$$C_{\text{outlet}} = \frac{\iint_{Z=0} C(r)\mathrm{dA}}{\iint_{Z=0} \mathrm{dA}} \tag{32}$$

The change in volumetric flow rate is assumed to be negligible, and thus, % CO_2 removal can be approximated by (31). COMSOL software can calculate this integral at the outlet of shell side and anywhere in the membrane contactor.

In Fig. 5, the CO_2 outlet concentration in the gas phase is plotted as a function of solvent flow rate or velocity for several solvents, and Fig. 6 illustrates the variation of the percentage removal of CO_2 as a function of liquid flow rate or velocity. It is clearly shown that as the solvent flow rate increases, mass transfer rate of carbon dioxide into the liquid increases. It could be attributed to this fact that increasing liquid velocity increases concentration gradients of CO_2 and solvent in the liquid–membrane interface; thus, the CO_2 outlet concentration in gas decreases (Fig. 5), and the percentage removal of CO_2 increases (Fig. 6).

The behavior of carbon dioxide absorbed in MDEA/MEA mixed amines with different compositions also illustrated in Figs. 5 and 6. It can be seen that adding a little amount of MEA into MDEA aqueous solution, the removal of CO_2 increases because the reaction rate constant of MEA with CO_2 is much higher than that of MDEA with CO_2. The transfer rate of carbon dioxide into the liquid increases as the concentration of MEA in mixed amines increases. As a result, the CO_2 outlet concentration in gas decreases, and the fractional removal of CO_2 increases with increasing concentration of MEA in MDEA/MEA aqueous solution.

It also can be seen from this figure that percentage removal of CO_2 reaches 100% at high liquid flow rates with MEA as absorbent. In a few separation devices, we can reach above 0.9, and it is very difficult along with consumption of much energy but HFMCs without consumption of much energy separate gas mixtures at high percentage removal. As an important result, this figure indicates that HFMCs have a great potential in the area of gas absorption specially CO_2 absorption.

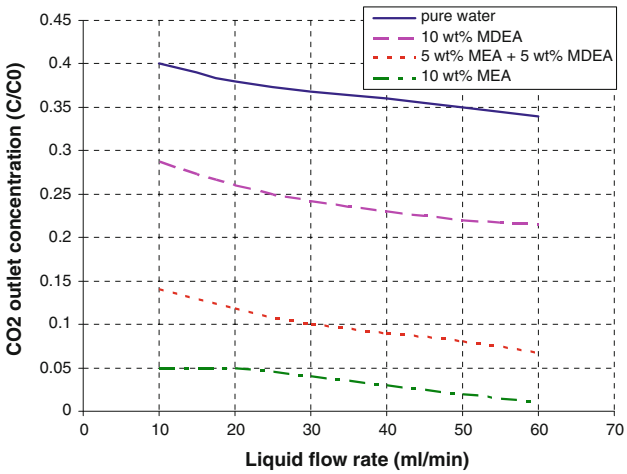

Fig. 5 Relationship between CO_2 outlet concentration in gas and liquid flow rate for various amines. Gas pressure = 121.3 kPa, temperature = 298 K, $n = 100$, $R = 0.5$ cm, $r_1 = 0.15$ mm, $r_2 = 0.20$ mm, $r_3 = 0.52$ mm, $L = 80$ cm, Gas flow rate = 100 ml/min, $Re_{out} = 3{,}500$

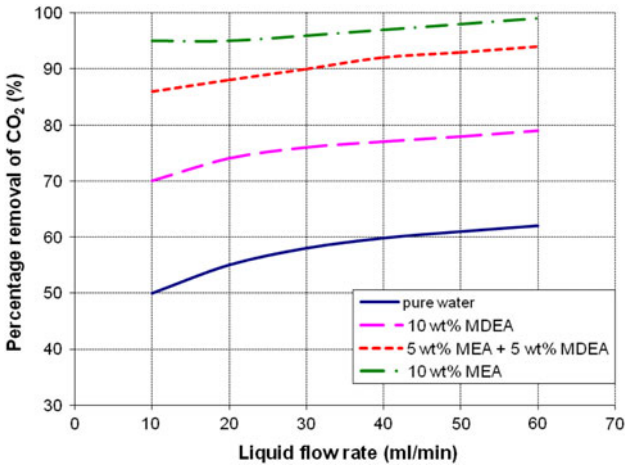

Fig. 6 Relationship between percentage removal CO_2 and liquid flow rate for various amines. Gas pressure = 121.3 kPa, temperature = 298 K, $n = 100$, $R = 0.5$ cm, Gas flow rate = 100 ml/min, $r_1 = 0.15$ mm, $r_2 = 0.20$ mm, $r_3 = 0.52$ mm, $L = 80$ cm, $Re_{out} = 3{,}500$

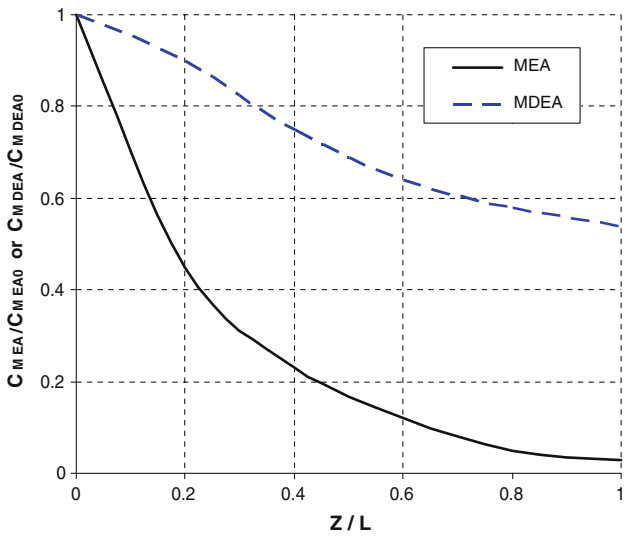

Fig. 7 Dimensionless concentration of amines versus dimensionless axial distance. Gas pressure = 121.3 kPa, temperature = 298 K, $n = 100$, $R = 0.5$ cm, Gas flow rate = liquid flow rate = 50 ml/min, $r/r_3 = 0.7$, $r_1 = 0.15$ mm, $r_2 = 0.20$ mm, $r_3 = 0.52$ mm, $L = 80$ cm, $Re_{out} = 3{,}000$

3.3 Concentration distribution of amine in the contactor

Figure 7 shows the dimensionless concentration of amines versus dimensionless axial distance in the membrane contactor. The modeling findings clearly indicate that the concentrations of amines decrease as the axial distance increases. Also, it can be seen that the differences of dimensionless concentration of MEA are much larger than that of MDEA. This indicates that the concentration gradient of MEA is much larger than that of MDEA due to the larger reaction coefficient of MEA with CO_2. Thus, the mass transfer flux of MEA is higher than that of MDEA in hollow-fiber membrane. Therefore, the consumption of MEA is larger than that of MDEA.

4 Model validation

4.1 Effect of gas and liquid velocities

The model developed in this study was then validated using the results obtained experimentally by Yan et al. [23]. They reported experimental results for separation of CO_2 from flue gas by a HFMC. In this section, the simulation results are compared with the experimental values to validate the mass transfer model. In this process, the CO_2 removal efficiency (η) and mass transfer rate (J_{CO_2}) were used to describe the process as follows [23]:

$$\eta = \frac{Q_{in} \times C_{in} - Q_{out} \times C_{out}}{Q_{in} \times C_{in}} \tag{33}$$

$$J_{CO_2} = \frac{(Q_{in} \times C_{in} - Q_{out} \times C_{out}) \times 273.15 \times 1000}{22.4 \times T_g \times S} \tag{34}$$

where η is the CO_2 removal efficiency, %; J_{CO_2} is the mass transfer rate of CO_2, mol/(m^2h); Q_{in} and Q_{out} are the gas flow rates at the inlet and the outlet, respectively, m^3/h; C_{in} and C_{out} are CO_2 volumetric concentrations in the gas phase at the inlet and outlet, respectively; T_g is the real temperature of the flue gas, K; and S is the gas–liquid interfacial area, m^2. C_{out} is calculated by integrating the local concentration at the outlet of shell side ($z = 0$). The module parameters of S. Yan et al.'s experiments are listed in Table 2.

The mass transfer rate of CO_2 along the contactor for different values of liquid velocities (the effect of convection term) is presented in Fig. 8. As mentioned earlier, increasing liquid flow rate (liquid velocity) increases the mass transfer rate of carbon dioxide to the tube side. The CO_2 removal efficiency along with the contactor for different values of gas flow rates is also presented in Fig. 9. As expected, the increase in the gas flow rate reduces the residence time of the gas phase in the membrane contactor, which in turn reduces the removal rate of CO_2.

The Figs. 8 and 9 also confirm that the model predictions are in good agreement with the experimental data for different values of gas and liquid velocities.

5 Conclusions

Absorption of CO_2 in hollow-fiber membrane contactors was studied theoretically in this work. A two-dimensional

Table 2 Module parameters of Yan et al. [23]'s experiments

Parameter	Value
Fiber inner diameter (μm)	344
Fiber outer diameter (μm)	442
Fiber porosity (%)	45
Module inner diameter (cm)	8
Fiber length (cm)	80
Number of fibers	7,000
Packing density (%)	21.4
Gas inlet pressure (kpa)	105
Temperature (K)	298

mathematical model was developed to describe chemical absorption of CO_2 in a gas–liquid hollow-fiber membrane contactor. The model predicts the steady-state solvent and CO_2 concentrations in the contactor by solving the conservation equations, including continuity and momentum. The model was developed for non-wetting conditions, taking into consideration axial and radial diffusions in the equations. The finite element method (FEM) was applied to solve the differential equations. The developed model was then validated using the results obtained from CO_2 removal from flue gas by amine aqueous solutions as the liquid solvent reported by Yan et al. [23]. Model predictions were in good agreement with the experimental data for different values of gas and liquid velocities. Absorption of CO_2 in amines aqueous solutions (MEA and MDEA) was simulated in this work. The MEA aqueous solution was better for absorption of CO_2 because of high solubility and

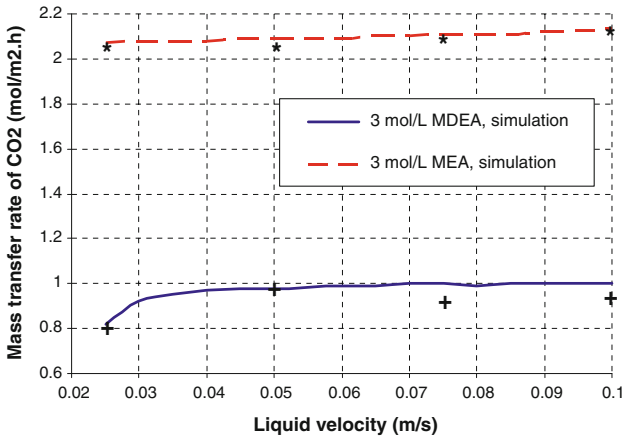

Fig. 8 Comparison of experimental results with simulation results for influence of liquid velocity on the mass transfer rate of CO_2. $U_g = 0.211$ m/s, $T_g = 298$ K, CO_2 volume fraction in feed gas = 14%, $T_l = 308$ K. *Plus symbol* experimental values for CO_2 absorption in MDEA, *asterisk* experimental values for CO_2 absorption in MEA [23]

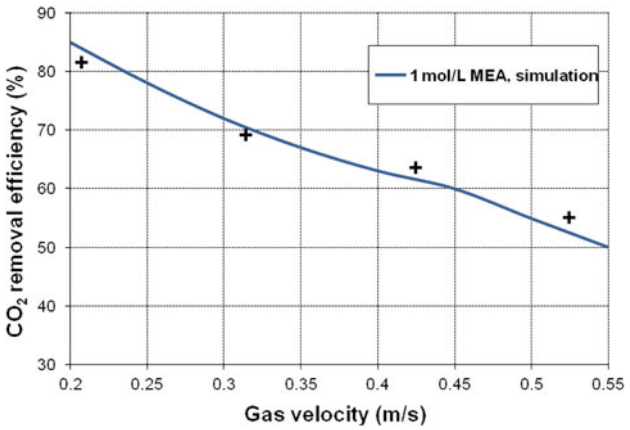

Fig. 9 Comparison of experimental results with simulation results for influence of gas velocity on the CO_2 removal efficiency. $U_l = 0.0503$ m/s, $T_g = 298$ K, CO_2 volume fraction in feed gas = 14%, $T_l = 308$ K. *Plus symbol* experimental values for CO_2 absorption in MEA [23]

reaction rate of CO_2 with MEA. The simulation results for the absorption of CO_2 in liquid solvents indicated that the removal of CO_2 increased with increasing liquid velocity in the tube side. Increasing gas velocity in the shell side has opposite effect.

References

1. Herzog H, Eliasson B, Kaarstad O (2000) Capturing greenhouse gases. Sci Am 182:72–79
2. Desideri U, Paolucci A (1999) Performance modeling of a carbon dioxide removal system for power plants. Energy Convers Manag 40:1899–1915
3. Herzog H (2001) What future for carbon capture and sequestration? ES&T 35:148A–153A
4. Gabelman A, Hwang ST (1999) Hollow fiber membrane contactors. J Membr Sci 159:61–106
5. Qi Z, Cussler EL (1985) Microporous hollow fibers for gas absorption. J Membr Sci 23:321–345
6. Kreulen H, Smolders CA, Versteeg GF, Van Swaaij WPM (1993) Microporous hollow fiber membrane modules. Ind Eng Chem Res 32:674–684
7. Falk-Pederson O, Dannstrom H (1997) Separation of carbon dioxide from offshore gas turbine exhaust. Energy Convers Manag 38:S81–S86
8. Kreulen H, Smolders CA, Versteeg GF, Van Swaaij WPM (1993) Microporous hollow fiber membrane modules as gas–liquid contactors. 2. Mass transfer with chemical reaction. J Membr Sci 78:217–238
9. Kumar PS, Hogendoorn JA, Feron PHM, Versteeg GF (2002) New absorption liquids for the removal of CO_2 from dilute gas streams using membrane contactors. Chem Eng Sci 57: 1639–1651
10. Karror S, Sirkar KK (1993) Gas absorption studies in microporous hollow fiber membrane modules. Ind Eng Chem Res 32:674–684
11. Zhang HY, Wang R, Tee Liang D, Hwa Tay J (2006) Modeling and experimental study of CO_2 absorption in a hollow fiber membrane contactor. J Membr Sci 279:301–310

12. Kim YS, Yang SM (2000) Absorption of carbon dioxide through hollow fiber membranes using various aqueous absorbents. Sep Purif Technol 21:101–109
13. Happel J (1959) Viscous flow relative to arrays of cylinders. AIChE J 5:174–177
14. Bird RB, Stewart WE, Lightfoot EN (2002) Transport phenomena, 2nd edn. Wiley, New York
15. Blauwhoff PMM, Versteeg GF, Van Swaaij WPM (1984) A study on the reaction between CO_2 and alkanolamines in aqueous solutions. Chem Eng Sci 39:207–225
16. Danckwerts PV (1979) The reaction of CO_2 with ethanolamines. Chem Eng Sci 34:443–446
17. Barth D, Tondre C, Lappai G, Delpuech J (1981) Kinetic study of carbon dioxide reaction with tertiary amines in aqueous solutions. J Phys Chem 85:3660–3667
18. Liao CH, Li MH (2002) Kinetics of absorption of carbon dioxide into aqueous solutions of monoethanolamine + *N*-methyldiethanolamine. Chem Eng Sci 57:4569–4582
19. Reid RC, Prausnitz JM, Poling BE (1987) The properties of gases and liquids. McGraw-Hill, New York
20. Wang YW, Xu S, Otto FD, Mather AE (1992) Solubility of N_2O in alkanolamines and mixed solvents. J Chem Eng 48:31–40
21. Hagewiesche PD, Aami SA, Hani Al-Ghawas A, Orville CS (1995) Absorption of carbon dioxide into aqueous blends of monoethanolamine and *N*-methyldiethanolamine. Chem Eng Sci 50:1071–1079
22. Versteeg GF, Van Swaaij WPM (1988) Solubility and diffusivity of acid gases (CO_2, N_2O) in aqueous alkanolamine solutions. J Chem Eng Data 33:29–34
23. Yan S, Fang M, Zhang W, Wang S, Xu Z, Luo Z, Cen K (2007) Experimental study on the separation of CO_2 from flue gas using hollow fiber membrane contactors without wetting. Fuel Process Technol 88:501–511
24. Gabelman A, Hwang ST, Krantz WB (2005) Dense gas extraction using a hollow fiber membrane contactor: experimental results versus model predictions. J Membr Sci 257:11–36